RAPORTTI A.2

A THERMAL MODEL FOR UPWARD FLAME SPREAD ON A COMBUSTIBLE WALL

Comparison of numerical calculations with large-scale experiments

Matti Kokkala
Djebar Baroudi

VTT Fire Technology
FIN - 02150 Espoo, FINLAND

DRAFT

December 1993

INTRODUCTION

In a large room with high walls the potential fire hazard of the wall linings depends to a great extent on the processes related to upward flame spread. The importance of the problem has been widely recognized and a considerable amount of related research has been carried out. However, the topic still remains one of the most important problems of fire physics [1].

Despite of the apparent simplicity of the fire scenario the problem is very complex. Various assumptions must be made when modelling upward flame spread. Unfortunately, efforts to verify the models with systematic large-scale experiments are scarce.

Large scale experiments in a room with combustible linings have shown that in a large room even a big fire may be "self extinguishing". For example, in the experiments of the EUREFIC research programme, substantial differences in the fire growth in rooms with heights of 2.4 m and 4.9 m were found. With a similar ignition procedure the materials which had exhibited flashover in a smaller 2.4 m high room did not do so in a larger 4.9 m high room. In some cases, even if the flames covered a considerable part of the ceiling of the room, the growth of the fire stopped and the flames retreated [2, 3].

The results immediately point out the importance of understanding whether the flame spread will accelerate or decelerate. In a large room where the fire in its early phase is not able to raise the gas temperature close to the ignition temperature of the materials, the question "to propagate or not to propagate" is more important than being able to predict the rate of propagation [4].

A review on upward flame spread has been made recently by, e.g., Fernandez-Pello [5]. Related references can be found there, and also in many of the references in this report.

In this publication we shall first present the basic concepts used to describe upward flame spread. A thermal of Parker [6] and Saito et al. [7]. The model offers a possibility for quantitative predictions of whether the flame spread is acceleratory or deceleratory. Our work benefits to a great extent on the recent work by Thomas and Karlsson [8] for solving the model equations. The model as such is almost identical with that of Karlsson [9, 10], who has found a reasonable agreement between the model calculations with results from large scale room corner tests. In this work we shall compare the calculations with simple upward flame spread tests with a gas burner as an ignition source at the base of a combustible wall.

WALL FLAMES AND THE UPWARD FLAME SPREAD

The fire scenario

Upward flame spread on a wall is schematically illustrated in figure 1. The lower edge of the material is the zero point of the coordinate x. The combustible lining has burned out in the region $x < x_b$. In the region $x_b < x < x_p$ the rate of pyrolysis is so high that we can say that the material is burning. The flame tip is assumed to be at $x = x_f$.

All the positions x_b, x_p, and x_f are understood as averages over a period of fluctuations, which are evident in the real flame spread processes.

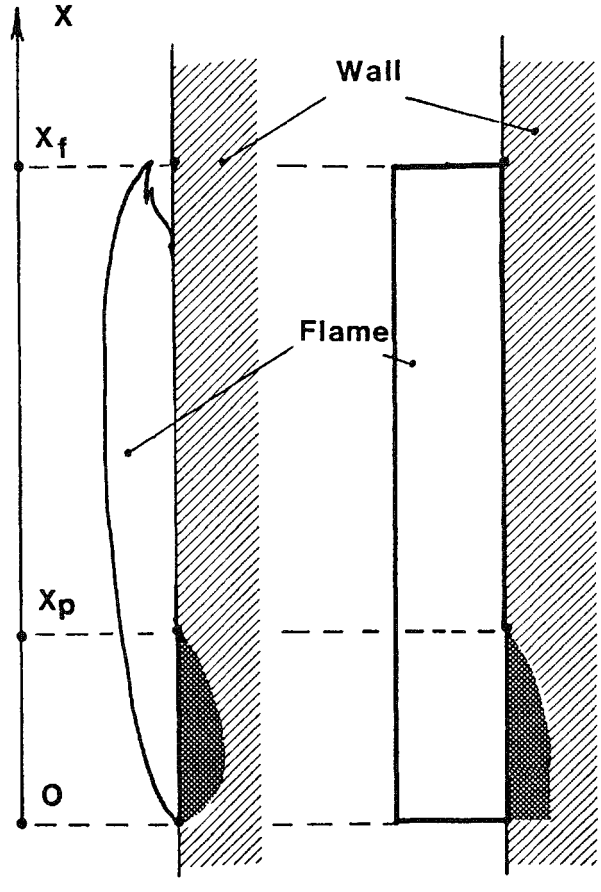

Fig. 1. a) A schematic picture of upward flame spread on a wall and b) a simplified picture for the calculation model.

Flame height correlations

It is generally agreed that the flame height defines the length scale of the preheating region. The height of a wall flame is generally presented as a function of the heat release rate in the form

$$x_f = k_f \, (\dot{Q}')^n \, , \tag{1}$$

where k_f is a constant depending on the properties of the surrounding atmosphere, $\dot{Q}'$ is the heat release rate per unit width of wall, and n is a dimensionless constant.

For example, Delichatsios [11] and Eklund [12] have derived expressions for the flame height resulting in $n = 2/3$ in which case

$$k_f = k' \, (C_p T_0 \rho_0 \sqrt{g})^{-\frac{2}{3}} \tag{2}$$

The dimensionless constant k' equals 4.65 in the model of Delichatsios and 5.0 in that of Eklund. Various experimental numbers are also available, which within the uncertainty of measurement are of the same order of magnitude.

In models of flame spread, the exponent $n = 2/3$ makes it impossible to find analytical solutions. Therefore, an approximation with $n = 1$, is often used. The flame height is then expressed as

$$x_f = K \dot{Q}' \equiv \dot{Q}' / \dot{E}'' \, , \tag{3}$$

where the constant K must be determined experimentally and where $\dot{E}''$ is the mean heat release density per unit area of the flame. The physical interpretation of the energy density is more easy to understand than the meaning of the constant K . Assuming that the mean heat release density of the flame is $\dot{E}''$, then the total heat release rate of the flame of width w and height x_f is $\dot{Q} = \dot{E}'' w x_f$. For example, the meaning of the parameter $K = 1 \times 10^{-5}$ m^2/W is not obvious whereas the meaning of the corresponding mean heat release density $E = 100$ kW/m^2 is clear.

In the case when the total rate of heat release includes both a part from the burner and from the wall linings, we usually add the two components. Thereafter we can apply either equation (1) or (3) to get the total flame length.

A problem when using the flame length scale is that various researchers define the flame length in different ways. The models of Delichatsios [11] and Eklund [12] calculate the flame tip as the point at which enough oxygen is entrained to burn all the fuel. Experimentally the flame length is defined either as the average length or as the maximum length of the visible flame.

Some authors have tried to correlate the flame length data by a function

$$x_f = x_{b0} + k(Q)^n, \tag{3}$$

where x_{b0} is the location of the burn out front [7]. Surprisingly enough, the fit of equation (1) usually seems better, although it definitely breaks out for high x_{b0} .

Pyrolysis front

The flame spread is usually understood as the propagation of the pyrolysis front x_p . The position of the pyrolysis front is in reality not well defined. For practical purposes, most of the flame spread models specify the pyrolysis front as the location at which the surface temperature of the material reaches an ignition temperature T_{ig} , i.e., a temperature at which the rate of pyrolysis is high enough to form a flammable mixture in the vicinity of the material. For most materials the ignition temperature is a reasonable characteristic parameter, because the rate of pyrolysis increases sharply with temperature.

In experiments one usually determines the position of the flame front with surface thermocouples. For materials like PMMA the method works well but especially for charring materials it involves considerable uncertainty due to difficulties in getting a good contact between the thermocouple and the surface.

Burn-out front

In principle, x_{b0} , the location of the burn-out front is well defined as the point were the flame goes out. For thin linings, burn out essentially occurs at the position where all of the lining has been pyrolysed. For charring materials extinction of the flames may occur even if the material is not completely consumed. Due to the char layer the rate of pyrolysis may decrease below a critical limit for flaming combustion. We shall use here the term 'burn-out front' for all types of materials to mean the position where flames are extinguished.

STATIONARY UPWARD FLAME SPREAD

In his awarded paper in the First International Symposium on Fire Safety Science, Hasemi presented derivations of the basic expressions for upward flame spread on both thermally thick and thermally thin materials [13]. In both cases Hasemi neglects the heat losses and the effects of charring surface of the surface prior to ignition. He assumes that the heat flux distribution above the pyrolysis front is known, but he does not make any assumptions on its functional form. The influence of the burning rate of the material is introduced into the flame spread velocity by scaling the heat flux distribution with the flame height.

The flame spread velocity for the thermally thick (semi-infinite) case is

$$V_p = \frac{(\int_0^\infty \dot{q}_w''(\xi+L_p)/\sqrt{\xi}\, d\xi)^2}{\pi k\rho c(T_{ig}-T_o)^2} \quad . \tag{5}$$

For of an exponentially decreasing flux, $\dot{q}_w'' = \dot{q}_o''\exp(-x/x_c)$, this reduces to

$$V_p = \frac{x_c \dot{q}_0''^2}{\pi k\rho c(T_{ig}-T_0)^2}, \tag{6}$$

as shown earlier by Sibulkin and Kim [14]. In the case the heat flux is constant for $x_p < x < x_f$ and zero for $x > x_f$, we get

$$V_p = \frac{4\ (x_f-x_p)\ \dot{q}_0''^2}{\pi k\rho c(T_{ig}-T_0)^2}. \tag{7}$$

For the thermally thin wall Hasemi finds

$$V_p = \frac{\int_0^\infty \dot{q}_w''(\xi+L_p)\exp(-h_i\xi/\rho cdV_p)d\xi}{\rho cd(T_{ig}-T_o)}. \tag{8}$$

The solution can be obtained by iteration. For an adiabatic (perfectly insulated) wall $h_i = 0$, and equation (8) reduces to

$$V_p = \frac{\int_0^\infty \dot{q}_w''(\xi+L_p)d\xi}{\rho cd(T_{ig}-T_o)}. \tag{9}$$

With the exponentially decreasing heat flux distribution one obtains

$$V_p = \frac{x_c \dot{q}_0''}{\rho cd\ (T_{ig}-T_0)}, \tag{10}$$

and with the constant heat flux,

$$V_p = \frac{(x_f-x_p)\ \dot{q}_0''}{\rho cd\ (T_{ig}-T_0)} \quad . \tag{11}$$

Equations (7) and (11) may be regarded as the basic equations of upward flame spread.

THERMAL MODEL FOR UPWARD FLAME SPREAD

Mathematical model

The thermal flame spread model of Parker [6] and Saito, Quintiere and Williams [7] is a generalization of equations (7) and (11) above. For both thermally thick and thermally thin materials the equations can be written in the form

$$\frac{dx_p}{dt} = \frac{x_f - x_p}{\tau_{ig}} \tag{12}$$

where τ is a characteristic ignition time at an irradiance level corresponding to the heat flux from the flame to the unignited surface. The model is valid only if $x_f > x_p$, because we are describing the spreading flame as a propagating ignition front. If $dx_p/dt < 0$ there is no ignition front. In the calculations we do not use this restriction, because we may also interpret τ as a time constant describing the development of fire.

We shall use the model here in the same way as Karlsson [9, 10] to predict the rate of heat release of the propagating fire. The positions of the pyrolysis front or the flame tip are only of secondary importance to us. They are effective parameters, which may be fitted in a way to produce agreement with experiments.

The input data to our calculations is obtained by running cone calorimeter tests at various heat flux levels. Because the flux level above the pyrolysis front varies as a function of time, we do not know *a priori*, which flux level is to be used. The time constant τ is the time to ignition. The flame height is calculated by integrating over the burning surface the rate of heat release of the product; the rate of heat release per unit area as a function of time is also obtained from the cone calorimeter tests. The time constant and the rate of heat release may be taken at different levels of exposure.

The flame spread problem is reduced to the mathematical problem of finding the function $x_p(t)$ solution of the initial value problem

$$\begin{cases} \dfrac{dx_p(t)}{dt} = \dfrac{x_f(t) - x_p(t)}{\tau_{ig}}, \quad t>0 \\ x_p(0) = x_{po}, \quad t=0 \\ x_f(t) = k_f \left(\dot{Q}'(t)\right)^n, \quad t>0,\ n>0,\ k_f>0 \end{cases} \tag{13}$$

where x_{po} is the initial pyrolysis height at the moment of ignition.

The total heat release rate per unit width of wall is a sum of the contributions of the burner and the burning wall:

$$\dot{Q}'(t) = \dot{Q}'_o(t) + \dot{Q}'_{fl}(t). \tag{14}$$

The contribution of the burner is known a priori. The unknown contribution of the burning material is calculated by integration as

$$\begin{aligned} \dot{Q}'_{fl}(t) &= x_{po}\dot{q}''(t) + \int_o^t \dot{q}''(t-\tau)\frac{dx_p(\tau)}{d\tau}\,d\tau \\ &= x_{po}\dot{q}''(t) + \int_o^t \dot{q}''(t-\tau)\,\frac{x_f(\tau)-x_p(\tau)}{\tau_{ig}}\,d\tau \end{aligned} \tag{15}$$

The initial value problem is non-linear because the unknown solution $x_p(t)$ is needed to calculate the flame height during the integration.

It is possible to solve the mathematical problem analytically for some special forms of cone calorimeter rate of heat release curve [7, 8, 15]. If we assume the rate of heat release curve to be of the form

$$\dot{q}'' = \dot{q}''_{\max}\exp(-t/\tau), \tag{16}$$

take the exponent $n = 1$, the flame spread may be accelerating, decelerating, or the spread may first accelerate and then come to a stop after a finite time. The various regions are functions of two dimensionless quantities: dimensionless ignition time $\gamma = \tau_{ig}/\tau$ and dimensionless heat release rate $a = k_f\dot{q}''_{\max}$. The boundaries of regions with different propagation behaviour are parabolic curves as seen in figure 2. More examples and discussion on the analytical solutions can be found in ref [15].

Numerical solution

To be able to solve the flame spread equations in general case, a numerical procedure is needed.

The initial value problem given in equation (12) is integrated using a conditionally stable explicit forward Euler method [18]. In this problem the stability condition requires a time step of integration $\Delta t \le 2\tau_{ig}$. The condition is easy to meet, because the relevant times to ignition are in the range 10 - 150 s.

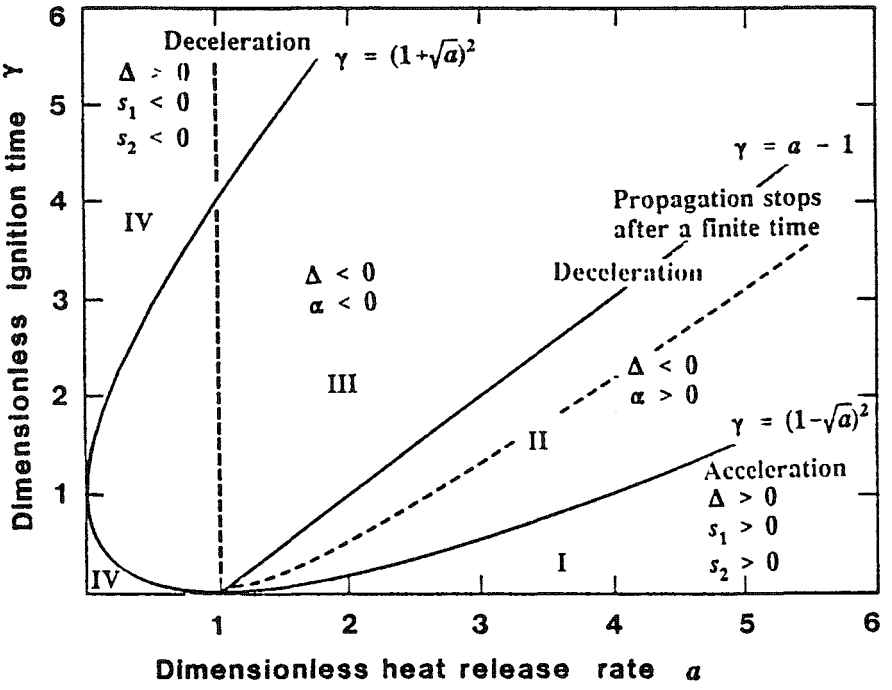

Fig. 2. Regions of various types of flame spread as a function of dimensionless heat release rate and dimensionless ignition time in the case of rate of heat release (RHR decays exponentially).

If $x_p(t_i)$ is known for a given t_i, equation (12) is discretized explicitly as

$$\begin{cases} \dfrac{dx_p(t_{i+1})}{dt} \approx \dfrac{x_p(t_{i+1}) - x_p(t_i)}{\Delta t_{i+1}} \\ \qquad\qquad = \dfrac{x_f(t_i) - x_p(t_i)}{\tau_{ig}}, \quad t_{i+1} > t_i,\ \Delta t_{i+1} = t_{i+1} - t_i \\ x_p(t_1) = \bar{x}_{po}\ ,\quad t_1 = 0 \\ x_f(t_i) = k_f \left(Q(t_i)\right)^n \end{cases} \tag{17}$$

From equation (17) we get

$$x_p(t_{i+1}) = \left(1 - \frac{\Delta t_{i+1}}{\tau_{ig}}\right) x_p(t_i) + \frac{\Delta t_{i+1}}{\tau_{ig}} x_f(t_i) \tag{18}$$

The contribution of the flame to the total heat release rate at time t_i is then integrated using a trapezoidal quadrature rule:

$$\begin{aligned} Q_{fl}(t_i) &= x_{po} q(t_i) + \int_o^{t_i} q(t_i - \tau) \frac{x_f(\tau) - x_p(\tau)}{\tau_{ig}} d\tau \\ &\approx x_{po} q(t_i) + \sum_{n=1}^{k=i} q(t_i - \tau_n) \frac{x_f(\tau_n) - x_p(\tau_n)}{\tau_{ig}} w_n \\ &= x_{po} q(t_i) + \sum_{n=1}^{k-1=i-1} q(t_i - \tau_n) \frac{x_f(\tau_n) - x_p(\tau_n)}{\tau_{ig}} w_n + \\ &+ q(0) \frac{x_f(t_i) - x_p(t_i)}{\tau_{ig}} w_i \end{aligned} \tag{19}$$

where the time interval from $\tau_1 = 0 = t_1$ to $\tau_k = t_i$ is discretized into k-1 intervals such that $\tau_n = t_1 + (n-1)h$ and the time step size $h = \tau_n - \tau_{n-1}$. The weights are $w_n = h$ for $n \neq 1$ or $n \neq k$ and otherwise $w_n = h/2$. The contribution of the burner is evaluated at time t_i as $Q_o(t_i)$.

The zero point of time is the moment when the wall behind the burner flame is ignited. Ideally, the burner flame and the wall flame would be similar, and we could assume the surface behind the burner flame to be ignited instantaneously. In practice, the burner flame may be of different thickness and we have to estimate the initial pyrolysis height independently. At time $t = t_1 = 0$ we have $x_p(0) = \bar{x}_p(0) > 0$. Consequently, the initial flame height is calculated as $x_f(0) = k_f\left(Q_o(0) + x_{po} q(0)\right)^n \geq x_p(0)$. The delay of ignition of the wall is taken into account as a shift of time after the numerical calculation has been completed.

The numerical procedure was verified by comparing against a known analytical solution. The results are shown in figure 3. We can easily see the excellent agreement.

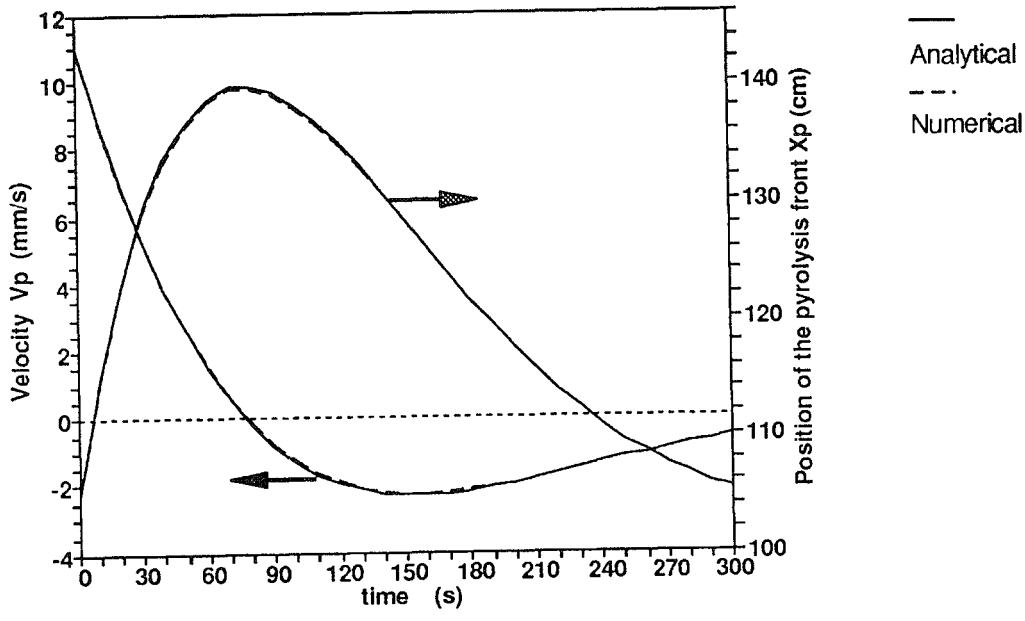

Fig. 3. Comparison of analytical and numerical solutions for an exponentially decaying heat release per unit area (eq. 16) and an exponent n = 1.

EXPERIMENTS FOR VALIDATING THE FLAME SPREAD MODEL

Test arrangement

In our project a series of large-scale tests were run to study upward flame spread on different wood products [16]. Tests were made both on 2.4 m high and 7.5 m high walls. The former system was equipped with instrumentation for the the measurement of rate of heat release, and all the comparisons in this paper shall be made with the tests on the lower wall.

The experimental arrangement is shown schematically in figure 4. The product to be studied was attached as a standard size (1.2 m wide) wall board on a vertical wood-framed sample holder. The backing of the board was either a 50 mm thick mineral wool or a 10 mm thick calcium silicate board.

The propane burner was a 1.2 m x 0.1 m and 0.1 m high sand-filled diffusion burner constructed in the same way as the square burners in the room/corner test standard. The burner was used with a propane output in the range of 40 kW - 300 kW. The output was kept constant with automatic control based on mass flow measurement in the feed line.

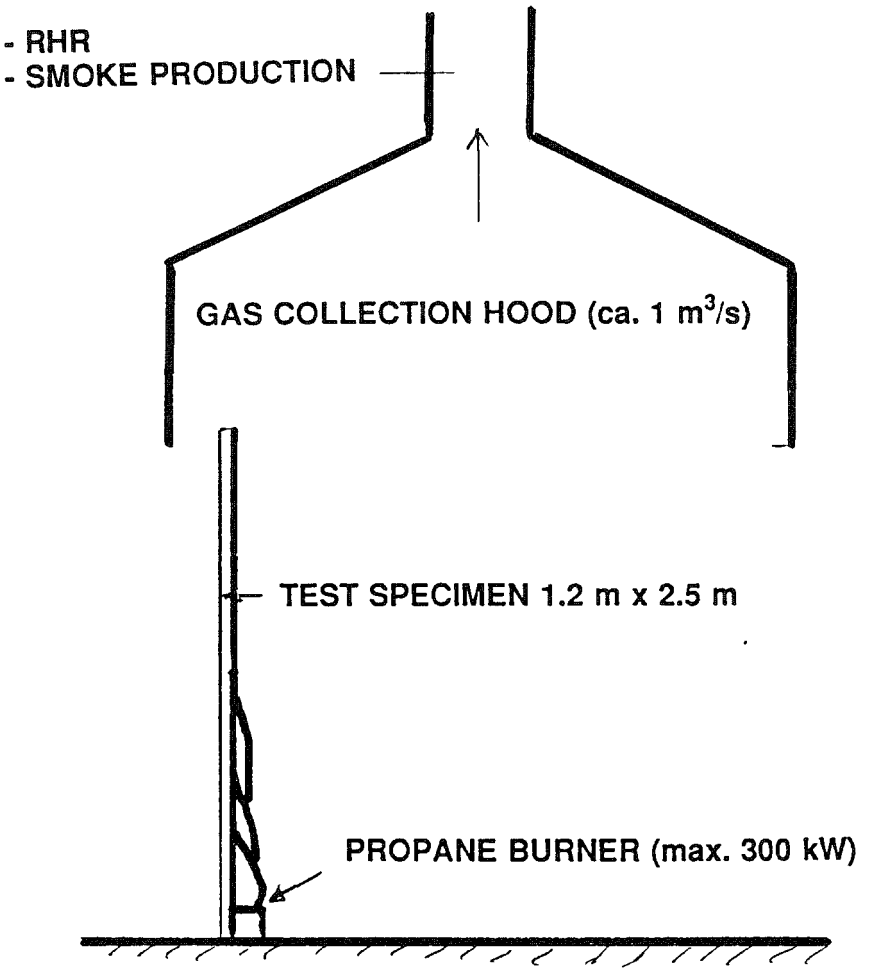

Fig. 4. Schematic picture of the upward flame spread test apparatus. See text for details.

The sample holder was part one of the three walls under a 3 m x 3 m gas collection hood used regularly as a furniture calorimeter or in the room/corner test as described, e.g., by Mangs et al [17]. The rate of heat release calorimetry was calibrated using the procedure defined in the room/corner test standard.

Results of experiments

We shall use here results of seven tests, which are listed in table 1. In addition tests were run on a noncombustible calcium silicate board to characterize the burner flame. The burning behaviour of the products was determined in the cone calorimeter on samples prepared in the same way as in the large scale tests.

Figure 5 shows the measured rate of heat release per unit area as a function of time in the cone calorimeter tests for irradiance levels of 25 kW/m^2 and 50 kW/m^2. Figure 6 shows the measured rate of heat release in the wall tests.

One of the key factors in the model is the flame height correlation. Figure 7 shows the flame height on a non-combustible wall as a function of burner output. A straight line fit appears to be the best possible choice, i.e. we can with good reason assume that the exponent $n = 1$. From the slope of the flame height fit we get $k_f = 0.60 \times 10^{-5}$ m^2/W or the rate of heat release per unit area of flame 166 kW/m^2.

More details of the tests and the test results will be published in ref. [16]. The data in the reference includes also surface and gas temperature measurements, heat flux measurements both into the wall and out of the burning wall. The measurements in the duct allow one to estimate also the rate of CO production and the convective energy flow into the duct.

Table 1. Test programme. All the other tests were run with a burner heat release rate of 100 kW, except in test T1002 the bunrer heat release rate was 70 kW.

Product	**Test code**	Time to ignition (s) 25 kW/m^2	50 kW/m^2	Maximum RHR (kW/m^2) 25 kW/m^2	50 kW/m^2
Particle board 11 mm on 50 mm mineral wool	**T2511**	105	34	165	224
Porous fibre board 10 mm on 50 mm mineral wool	**T0412**	37	9	137	185
Particle board 11 mm on 15 mm calcium silicate board	**T2312**	103	31	170	227
Textile wall cov. + calcium silicate board on 50 mm mineral wool	**T1301**	no ign.	17	no ign.	234
Particle board 11 mm on 50 mm mineral wool	**T1002**	105	34	165	224
Wood 9 mm; horizontal grooves on 50 mm mineral wool	**T0203**	158	13	132	233
Wood 9 mm; vertical grooves on 50 mm mineral wool	**T0903**	158	13	132	233

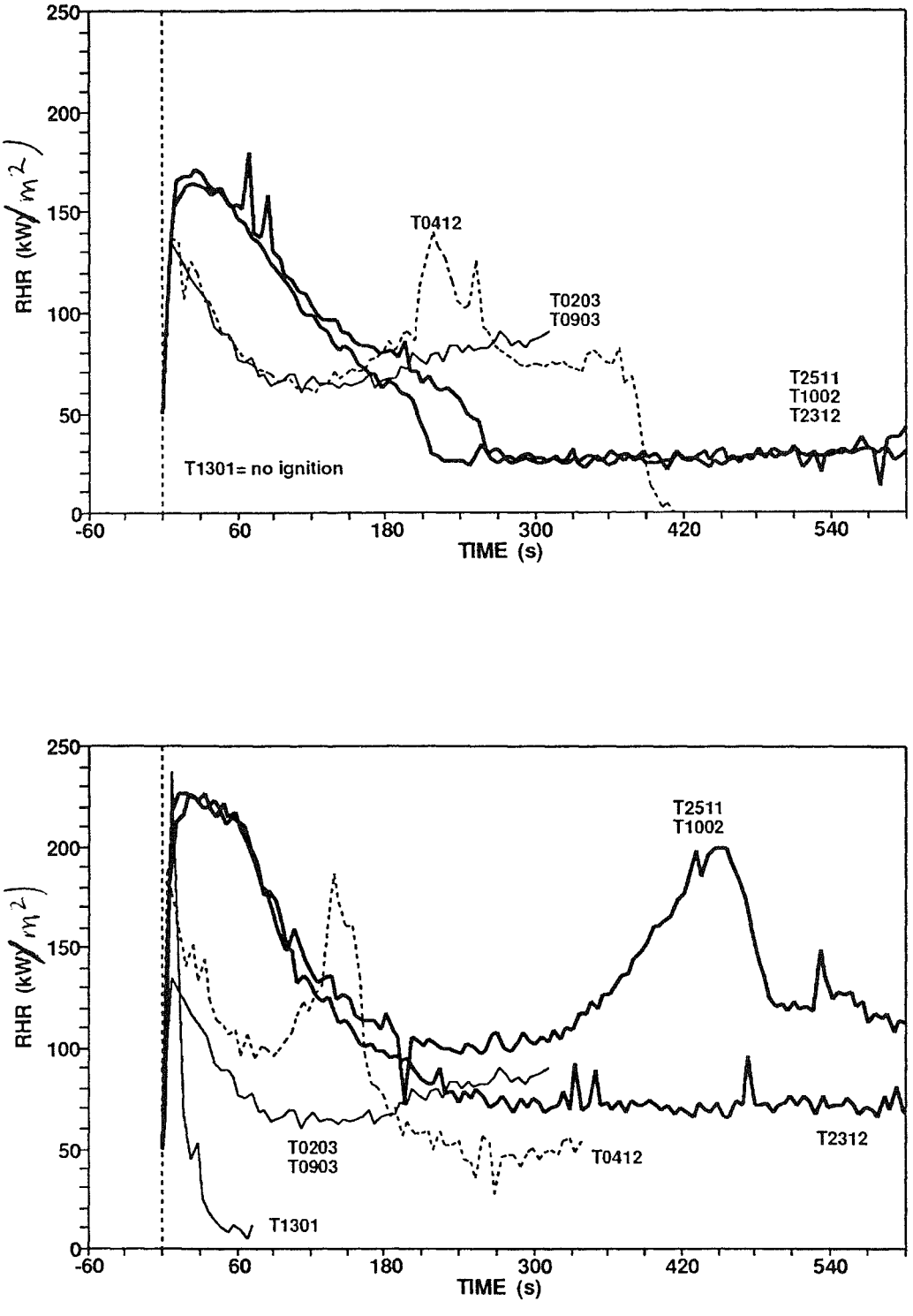

Fig. 5 Measured rate of heat release per unit area as a function of time in the cone calorimeter tests for irradiance levels of a) 25 kW/m^2 and b) 50 kW/m^2. For product identification, see table 1.

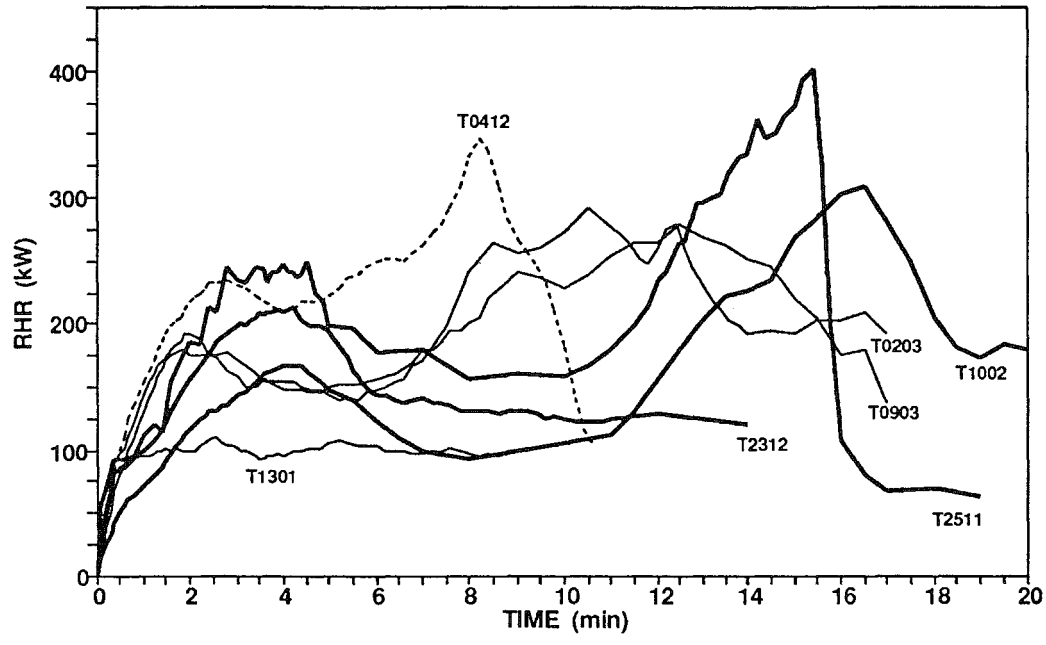

Fig. 6. Measured rate of heat release as a function of time in the wall fire tests on 1.2 m wide and 2.4 m high specimens. For product identification and test conditions, see table 1.

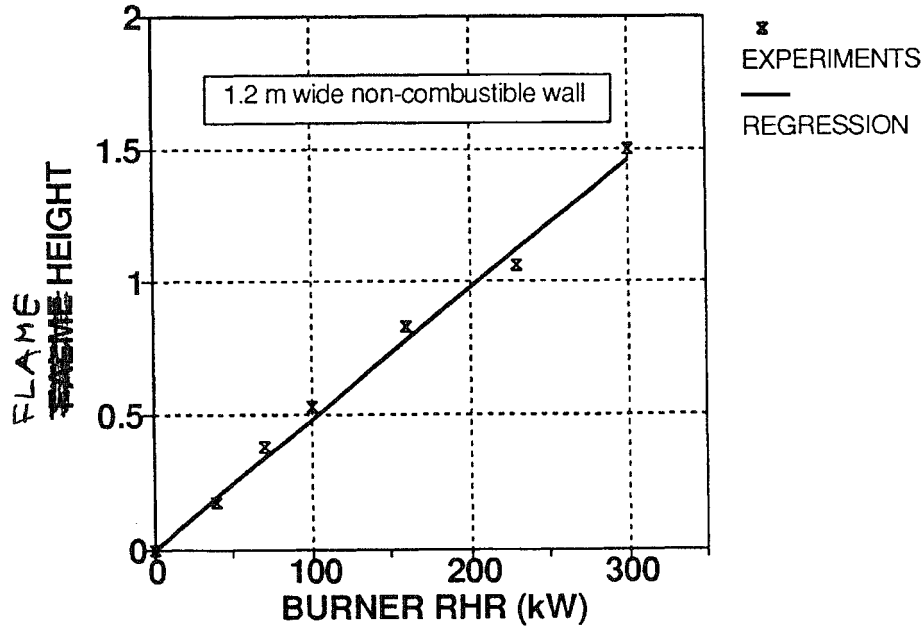

Fig. 7. Measured flame height on a noncombustible wall as a function of the propane burner output. The burner is 1.2 m wide and 0.1 m deep.

COMPARISON OF CALCULATIONS WITH EXPERIMENTAL DATA

After a few rounds of trial and error, the following assumptions were fixed for later calculations.

a) The initial pyrolysis height was taken as 40 % of the measured flame height, i.e 0.2 m for the 100 kW and 0.14 m for the 70 kW burner heat release rates.

b) The flame height coefficient $k_f = 0.65 \times 10^{-5}$ m^2/W. This values is close to that of the burner flame only, but it is only about 65% of the value for the wall flames. It appears, however, that the burner flame is dominating the early fire spread, and the values corresponding to the burner are more relevant.

c) The initial ignition is assumed to take place at the time of ignition at an irradiance level of 50 kW/m^2. This level is found behind the continuous flame close to the base of fire. This value is used as a shift of calculated heat release rates when compared with experiments.

d) The time to ignition in the model is taken at an irradiance level of 25 kW/m^2 as the time when the rate of heat release per unit area reached 50 kW/m^2. These times to ignition are very close to those observed in the tests. With the values taken at the irradiance level of 50 kW/m^2 the calculated fire spread rate turned out to be too fast.

e) The rate of heat release from the cone is also taken at a level of 25 kW/m^2. A heat flux of this order of magnitude was measured behind the wall flame above the tips of the thicker burner flame. heat flux levels of the same order of magnitude have been found also by Hasemi et al [19]. Because much of the spreading took place behind the burner flame, we expected a higher flux level to be more appropriate. However, in the wall tests the rate of heat release per unit area **was** of the order of that in the cone calorimeter at the lower irradiance level. The use of the heat release data from the 50 kW/m^2 would require the flame length coefficient k_f to be forced unrealistically low.

Figures 8 to 14 show the calculated heat release rates and flame lengths.

For the particle board on mineral wool (figures 8 and 9) the model is able to predict the first peak of heat release rate with very good accuracy. The effect of changing the burner out put (70 kW or 100 kW) is predicted very well.

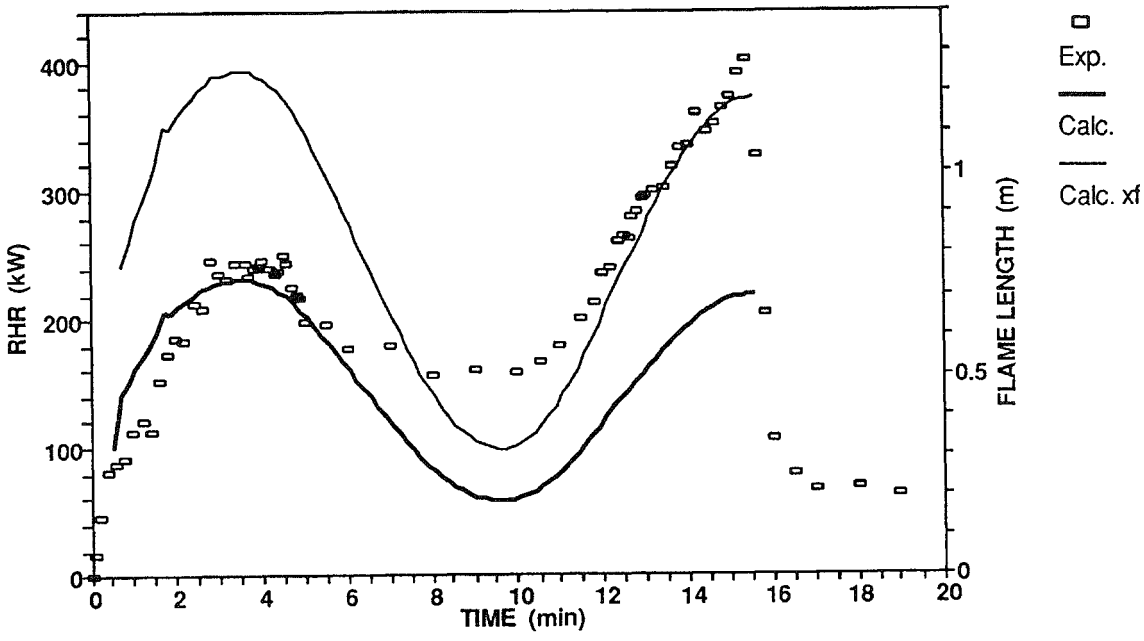

Fig. 8. Measured and calculated rates of heat release and the calculated flame length as a function of time in the test ***T2511: particle board*** *on mineral wool and a* ***100 kW*** *ignition source.*

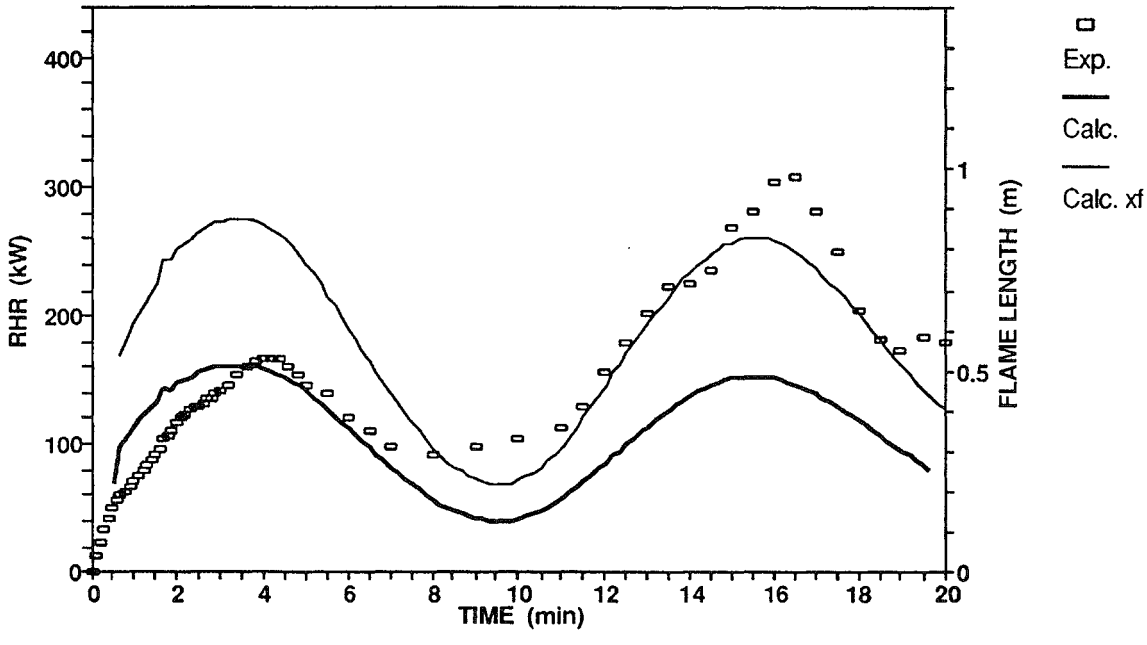

Fig. 9 Measured and calculated rates of heat release and the calculated flame length as a function of time in the test ***T1002: particle board*** *on mineral wool and a* ***70 kW*** *ignition source.*

After the first peak the calculated heat release rates decrease unrealistically below the level of the burner output. One may note, however, that in this phase the assumptions of the model are not valid. Despite of the problem with the deep valley in the curve, the model seems to be able to predict the second peak of heat release, but only qualitatively.

The first peak is obtained reasonably well also in the case of particle board with the conducting calcium silicate board as a backing (figure 10), but the second peak is much lower than calculated for the board with mineral wool backing. An evident correction to the numerical model would be to force the rate of heat release to stay at least at the level of the burner. This would possibly bring the second peak of the heat release curve closer to the measured values.

In the case of the porous fibre board (figure 11) the model is able to reproduce the measured heat release rate curve with good accuracy, although the first peak is slightly out of phase. In the test the wall burned for a longer period, but that may be due to the early burn through in the tests.

In the case of the textile wall covering (figure 12) there is a sharp peak soon after ignition in the calculated heat release curve, which was not seen in the tests. The model brings the heat release rate down to the stable level of the burner output.

For wood the cone calorimeter did not in this case show the characteristic two peak behaviour of wood products. The reason for that is unknown. Consequently, the calculated curve (figure 13) does not show the two phase flame spread observed in the large scale tests.

Figure 14 is an example of the effect of taking the cone calorimeter heat release rate at a level of 50 kW/m^2. The model clearly overpredicts the experimental result. The error could be compensated by increasing the assumed time to ignition, which here is taken at an irradiance of 25 kW/m^2, or by decreasing the flame length coefficient to a lower value.

The calculated flame lengths are systematically shorter than those observed during the tests. The reason for that is that the flame length coefficient has been taken to correspond to a value measured for the burner flame which is thicker than the flame from the burning surface.

The results of the model calculations are very promising. However, further work is needed to systematically study the sensitivity of the results on the input parameters. With different parameter combinations one might, e.g., be able to use the cone calorimeter data taken at an irradiance level other than 25 kW/m^2. For this work data was also recorded at an irradiance level of 50 kW/m^2, but that is apparently too high a level for our purposes. An intermediate level like 35 kW/m^2 would be worth trying, because the measured heat fluxes behind the spreading flame were of that order.

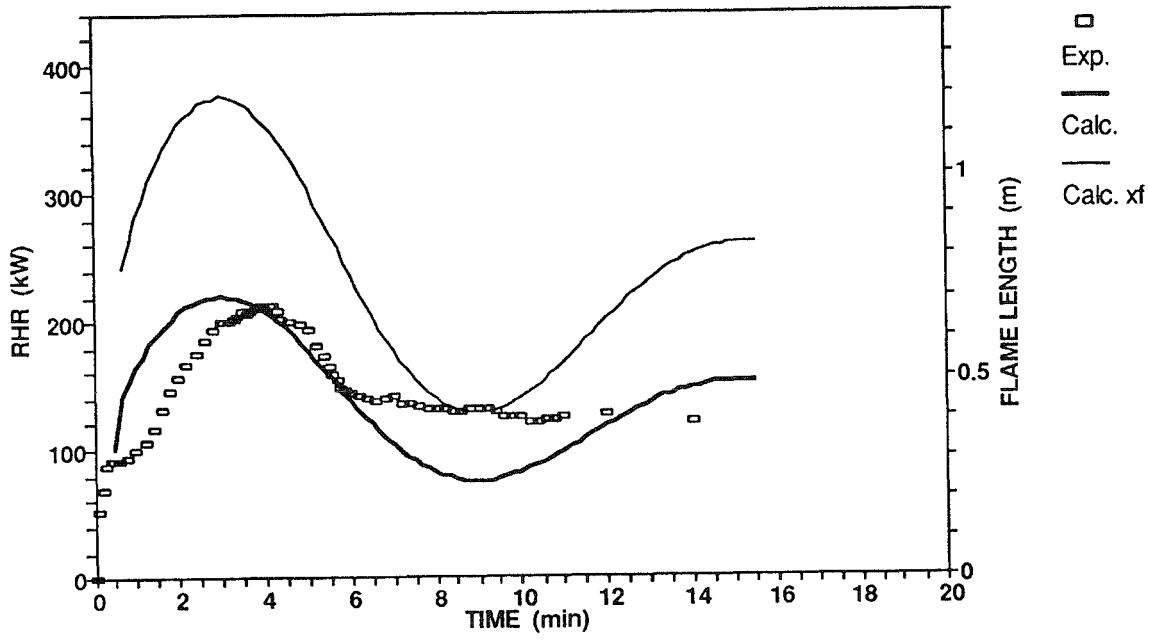

Fig. 10. Measured and calculated rates of heat release and the calculated flame length as a function of time in the test ***T2312: particle board on calcium silicate board*** *and a* ***100 kW*** *ignition source.*

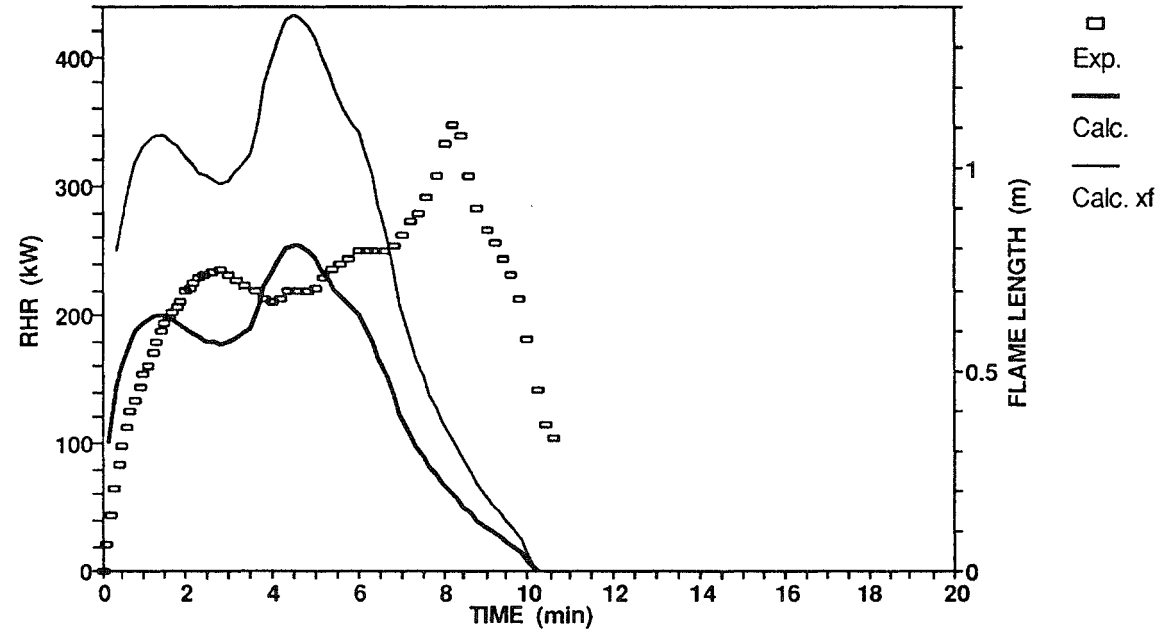

Fig. 11. Measured and calculated rates of heat release and the calculated flame length as a function of time in the test ***T0412: porous fibre board*** *on mineral wool and a* ***100 kW*** *ignition source.*

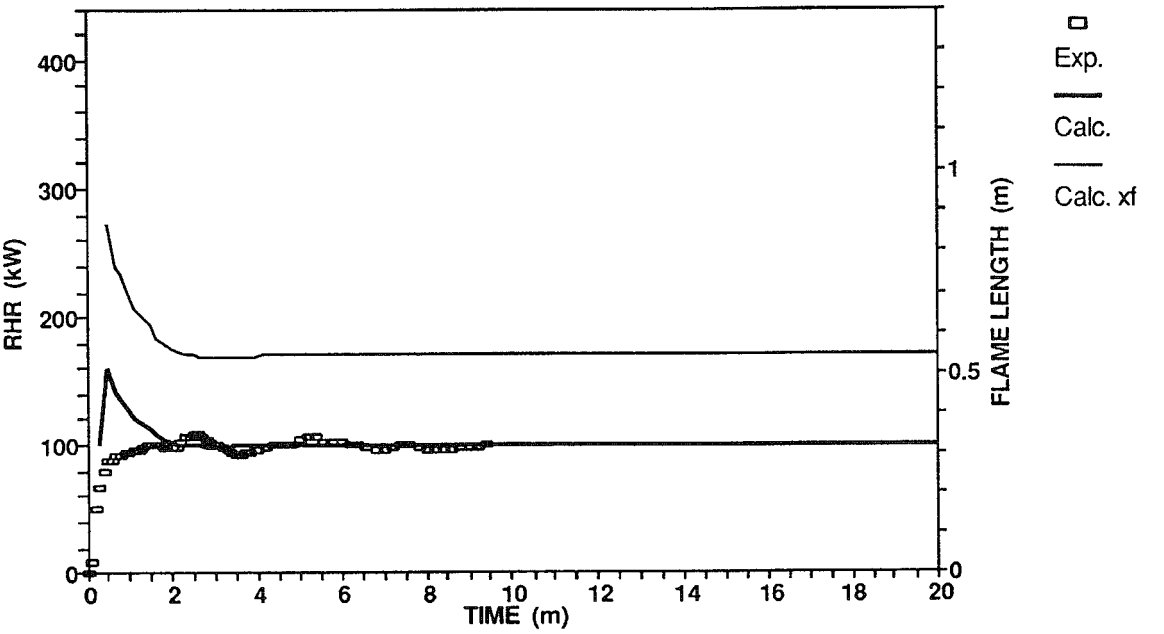

Fig. 12. Measured and calculated rates of heat release and the calculated flame length as a function of time in the test ***T1301: textile wall covering*** *on calcium silicate board and a* ***100 kW*** *ignition source.*

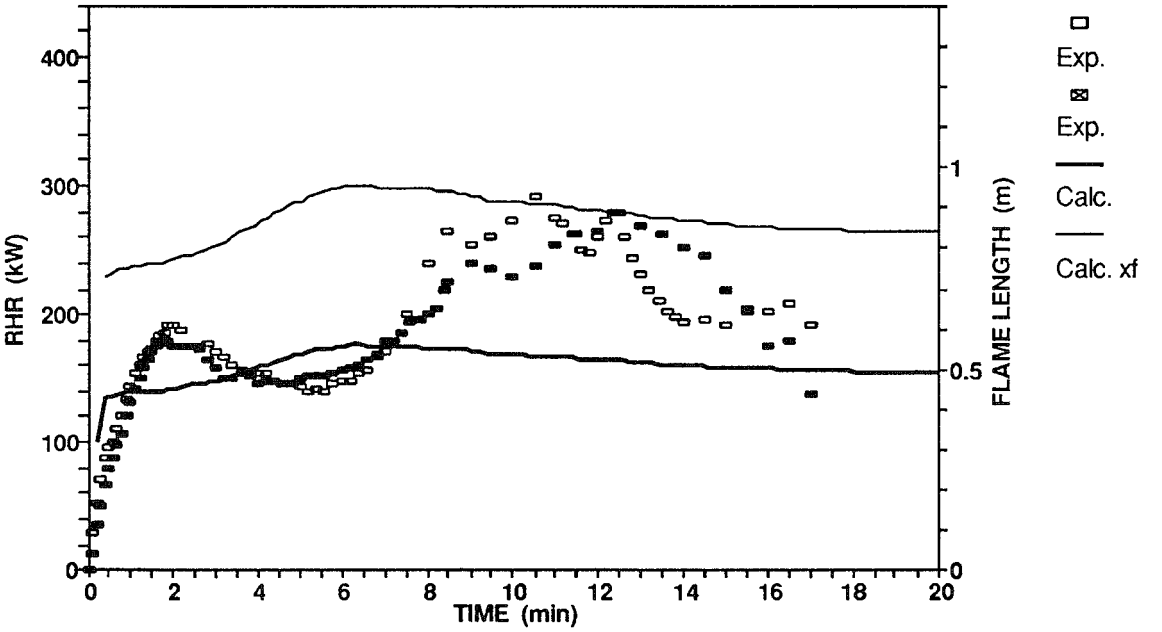

Fig. 13. Measured and calculated rates of heat release and the calculated flame length as a function of time in the test ***T0203*** *(horizontal grooves) and T0903 (vertical grooves):* ***9 mm thick pine*** *tongue and groove boards on mineral wool and a* ***100 kW*** *ignition source.*

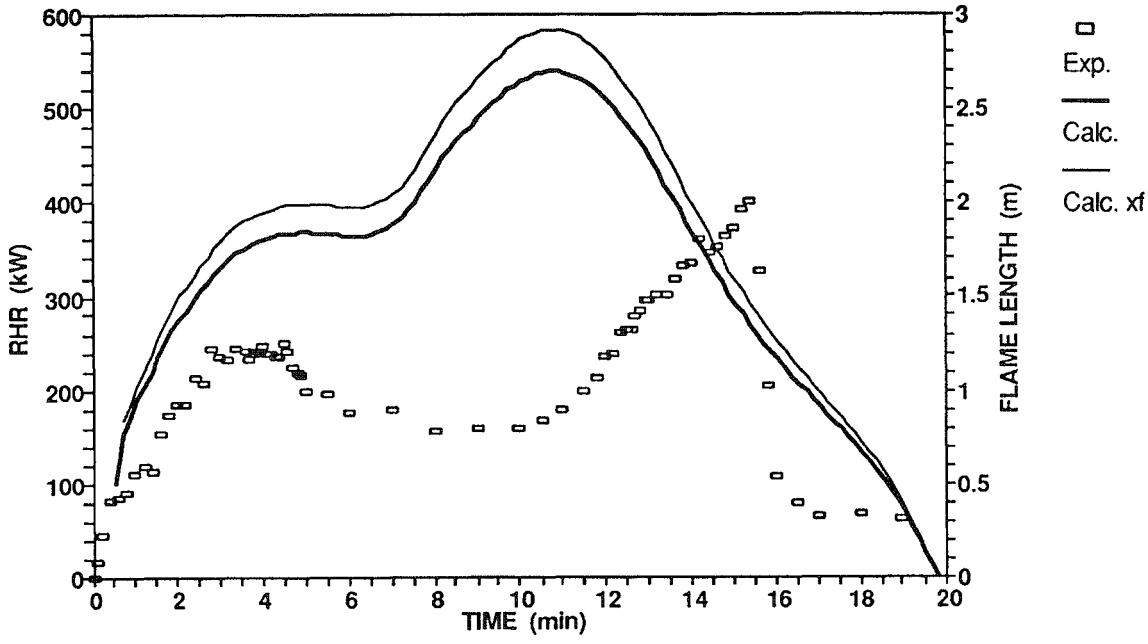

Fig. 14. Measured and calculated rates of heat release and the calculated flame length as a function of time in the test T2312: particle board on calcium silicate board and a 100 kW ignition source. The cone calorimeter data is taken here at 50 kW/m^2 while on all the previous figures it was taken at 50 kW/m^2.

APPLICATION OF THE FLAME SPREAD MODEL FOR HAZARD ASSESSMENT

The model described above was proven to be able to predict with reasonable accuracy the rate of heat release of a fire spreading on a wall. As an application of the model, information of whether the spreading fire is to go out on its or to grow in such a way that a flashover is possible, would be of great practical importance.

For a flashover to occur, a critical level of rate of heat release can be usually determined, if the geometry and the thermal properties of the room are known. One of the simplest ways is to use the correlations of McCaffrey et al [20] to obtain

$$\dot{Q}_{cr} = 15800 W^{1/2} K^{1/2} m^{5/4} \quad (h_k A_T W H^{3/2})^{1/2} \tag{20}$$

where the heat transfer coefficient is $h_k = (k\rho c/t)^{1/2}$, in W/mK with t the time from the moment of ignition, A_T the total surface area (floor, ceiling, walls) in the room excluding the openings, and W and H the width and the height of the

opening, respectively. The correlation is essentially valid for steady state conditions. Because our flame spread model does not take into account any feed back effects in the room, a reasonable safety factor must be used. The coefficient in equation (20) has been fixed so that the condition for flashover is correct for typical wood products in the standard room/corner test (2.4 m x 3.6 m x 2.4 m high room). Due to lack of experimental data, we recommend one to use a safety factor in the range 2 - 3 when significantly larher or higher rooms.

Figure 15 describes the process of using the flame spread model to determine whether a fire on wall linings is able to cause a flashover in the room. Because no calibrations against realistic ignition sources in large rooms have not been made, the method must be used with great care. further validation of the method is definitely needed.

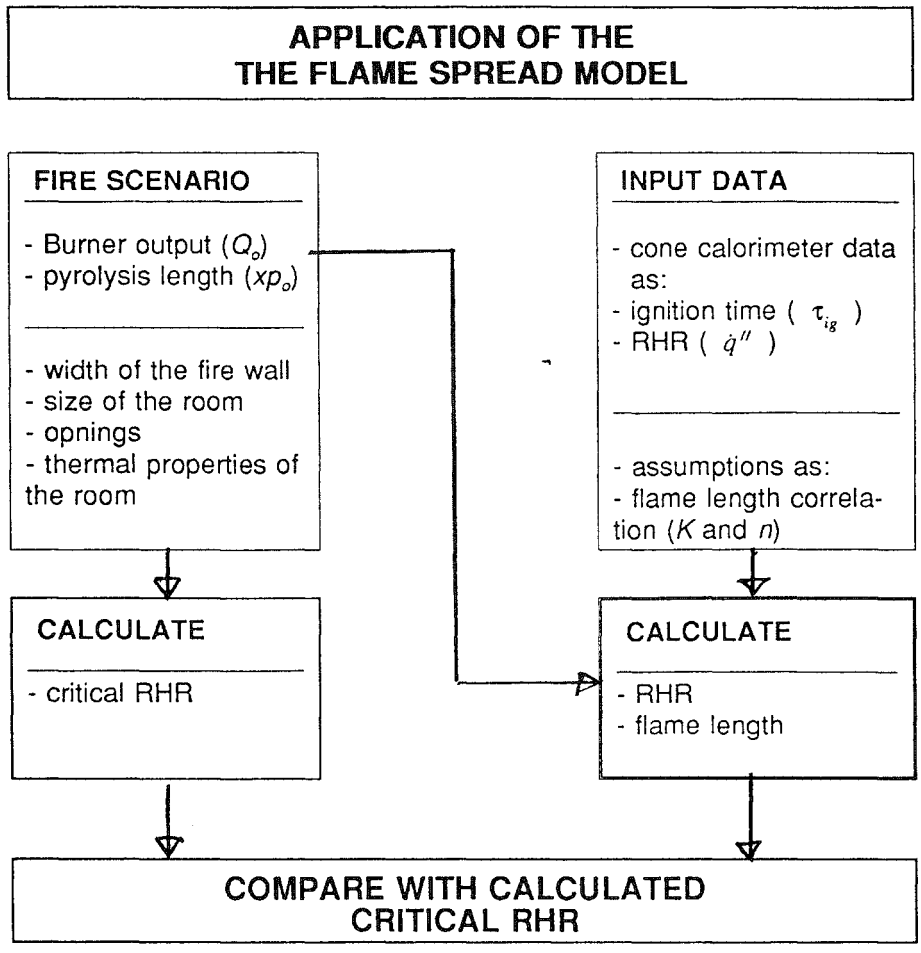

Fig. 15. Application of the flame spread model for hazard assessment. The calculated rate of heat release must be compared to a critical rate of heat release depending on the size, openings, and thermal properties of the room of fire origin.

REFERENCES

1. Thomas, P. H., Fire science research & engineering into the 1990's. Proc. of Interflam '90 held at Univ. of Kent, Canterbury, England, 3 - 6 September 1990, London 1990, Interscience Communications Ltd, P. 345.

2. Söderbom, J., Large scale fire experiments according to ISO DIS 9705, Project 4 of the EUREFIC fire research programme, Borås, Sweden 1991, Swedish National Testing and Research Institute, SP Report 1990:41, 20 p.

3. Kokkala, M., Göransson, U., and Söderbom, J., Five large-scale room fire experiments, Project 3 of the EUREFIC fire research programme, Espoo, Finland 1992, Technical Research Centre of Finland, VTT Publications 104, 60 p. + app. 49 p.

4. deRis, J., Discussion at the Wall-fire workshop, 12 - 13 October 1988, National Institute of Standards and Technology, Gaithersburg, MD, USA, (notes by H. Mitler).

5. Fernandez-Pello, A. C. Fire propagation in concurrent flows. Gaithersburg, MD, USA 1990, National Institute of Standards and Technology, NIST-GCR-90-586, 132 p.

6. Parker, W.J., An assessment of correlations between laboratory and full scale experiments for the FAA Aircraft Fire Safety Program, Part. 3; ASTM E 84, Gaithersburg, MD, USA 1982, National Bureau of Standards and Technology, NBSIR 82-2564, xxx p.

7. Saito, K., Quintiere, J. Q. and Williams, F. A. Upward turbulent flame spread. Fire Safety Science - Proceedings of the First International Symposium. Gaithersburg, MD, 7 - 11 Oct., 1985. New York, 1985, Hemisphere Publ. Corp. Pp. 75 - 86.

8. Thomas, P. H. and Karlsson, B. On upward flame spread. Lund, Sweden 1991, Lund University, Department of Fire Safety Engineering, SE-LUTVDG/TVBB-3058, 22 p.

9. Karlsson, B., Modeling fire growth on combustible lining materials in enclosures, Lund, Sweden 1992, Lund University, Department of Fire Safety Engineering, TVBB-1009, 201 p. (Ph.D. thesis).

10. Karlsson, B., A mathematical model for calculating heat release rate in the room corner test, Fire Safety Journal, 20, 1993, pp. 93 - 113.

11. Delichatsios, M. A. Critical conditions for sustained burning and flame propagation on vertical charring walls. New York, NY, USA 1983, The American Society of Mechanical Engineers, Paper 83-WA/HT-64, 6 p.

12. Eklund, T. I. A vortex model for wall flame height. Journal of Fire Sciences, 4(1986), pp. 4 - 14.

13. Hasemi, Y. Thermal modeling of upward wall flame spread. Fire Safety Science - Proceedings of the First International Symposium. Gaithersburg, MD, 7 - 11 October 1985. New York 1985, Hemisphere Publ. Corp. Pp. 87 - 96.

14. Sibulkin, M., and Kim, J. The dependence of flame propagation on surface heat transfer II, Upward burning. Combustion Science and Technology, 17, 1977, p. 39.

15. Baroudi, D. and Kokkala, M., Analysis of upward flame spread, Project 5 of the EUREFIC fire research programme, Espoo 1992, Technical Research Centre of Finland, VTT Publications 89, 49 p.

16. Kokkala, M., Parker, W.J., Mikkola, E., Immonen, M., Juutilainen, H., and Manner, P., Large-scale upward flame spread tests on wood products, to be published.

17. Mangs, J., Mikkola, E., Kokkala, M., Söderbom, J., Stenhaug, E., and Østrup, I., Room/corner tests round robin, Project 2 of the EUREFIC fire research programme, Espoo 1991, Technical Research Centre of Finland, VTT Research Reports 733, 36 p + app. 26 p.

18. Scheid, F., Analyse numérique, cours et problèmes, Serie Schaum, deuxième tirage. McGraw-Hill, Paris, 1987. 423 p.

19. Hasemi, Y., Yoshida, M., and Yasui, N., Upward flame spread along charring materials: model, model verification and application to material fire safety performance, Building Research Institute, Tsukuba, Japan 1992, unpublished draft, 10 p.

20. McCaffrey, B.J., Quintiere, J.Q., and Harkleroad, M.F., Estimating room fire temperatures and the likelihood of flashover using fire test data correlations, Fire Technology, 17, 2, 1981, pp. 98 - 119.